Available online at www.sciencedirect.com
SCIENCE DIRECT
Journal of Power Sources 148 (2005) 72–77
JOURNAL OF POWER SOURCES
www.elsevier.com/locate/jpowsour

Improvement of the high-rate discharge properties of $LiCoO_2$ with the Ag additives

Shahua Huang [a,b], Zhaoyin Wen [a,b,*], Xuelin Yang [a,b], Zhonghua Gu [a], Xiaohe Xu [a]

[a] *Shanghai Institute of Ceramics, Chinese Academy of Sciences, Shanghai 200050, PR China*
[b] *Graduate School, Chinese Academy of science. 1295 DingXi Road, Shanghai 200050, PR China*

Received 22 October 2004; received in revised form 14 January 2005; accepted 1 February 2005
Available online 23 March 2005

Abstract

The powders of $LiCoO_2$/Ag composite were prepared by thermal decomposition of $AgNO_3$ added to commercial $LiCoO_2$ powders and were examined on their electrochemical performance with particular attention to their high-rate charge–discharge cycling properties as cathode materials for lithium-ion batteries. X-ray diffraction (XRD), scanning electron microscopy (SEM), ac impedance, CV and charge–discharge cycles were used to evaluate the $LiCoO_2$/Ag composite powders. It was shown that the Ag additive effectively increased the electrical conductivity of the $LiCoO_2$ and decreased the polarization of cathode, and marvellously improved the high-rate discharge capacity and cycling stability of $LiCoO_2$.

Keywords: Lithium-ion batteries; High-rate discharge properties; $LiCoO_2$; Ag; Additive

1. Introduction

High-rate capability of lithium-ion batteries especially of cathode materials have attracted growing attentions in the past few years due to their potential applications in the electric vehicles (EV) [1,2]. The layer structured oxide $LiCoO_2$ is the earliest founded lithium metal oxide used as cathode material. Good performance and stability make it the main commercially used cathode material, despite toxicity and high cost [3–6].

For commercial products, 3C is usually the highest charge–discharge rate and 1C is the commonly used rate. Decreasing the particle size of the cathode material and extending its surface area are ideal ways to increase the activity of the electrode material [7–10]. In addition, thin-film [11] and highly porous [2] electrodes have been reported to show better rate capability than conventional electrodes. However, conductive fillers are routinely added to lithium-ion battery electrodes to construct conductive percolation network in order to achieve full electrode utilization [12–14] and increase battery power [14,15]. In our previous study, we found that the Ag additive effectively improved the discharge capacity and cycling stability of $Li_4Ti_5O_{12}$ at a rate as high as 4C [16], Son et al. ever reported improved cycling performance and capacity of $LiMn_2O_4$ by Ag coating based on a chemical process [17].

In this paper, we developed a technique to easily make composite of commercial $LiCoO_2$ and Ag metal, particular attention will be paid to the high-rate cycling discharge performance. X-ray diffraction (XRD) analysis and scanning electron microscopy (SEM) observations as well as electrochemical cycling test will be used to characterize the electrode materials.

2. Experimental

2.1. Preparation of the $LiCoO_2$/Ag composite electrode

Commercial $LiCoO_2$ powder from Huitong Co., China, was used as the precursor for the $LiCoO_2$/Ag composite.

* Corresponding author. Tel.: +86 21 5241 1704; fax: +86 21 5241 3903.
E-mail address: zywen@mail.sic.ac.cn (Z. Wen).

0378-7753/$ – see front matter © 2005 Elsevier B.V. All rights reserved.
doi:10.1016/j.jpowsour.2005.02.002

$AgNO_3$ (9 wt%) and the commercial $LiCoO_2$ (91 wt%) powder were homogeneously mixed by planetary ball milling for 4 h with alcohol as solvent and then heated at 80 °C for 12 h to evaporate the alcohol. Samples were heated in a muffle furnace at 50 °C for 2 h in air, and then cooled down to room temperature naturally.

The composite electrodes were made of the $LiCoO_2$/Ag powders (85 wt%), acetylene black (7 wt%) and polyvinylidene fluoride (PVDF) binder (8 wt%) homogeneously mixed in *N*-methyl pyrrolidinone (NMP) solvent by planetary ball milling and then coated uniformly on an aluminum foil. Finally, the electrode was dried under vacuum at 100 °C for 10 h before electrochemical evaluation.

2.2. Measurements

Phase analysis of the Ag doped $LiCoO_2$ was performed on a Guinier–Hägg camera by a powder diffraction method using Cu $K\alpha_1$ radiation as the radiation source ($\lambda = 1.5405$ Å) and Si as an internal standard. The obtained films were evaluated with a computerized scanner system. The cell dimensions of the Ag composited $LiCoO_2$ phase were determined by means of the PIRUM program based on the Guinier–Hägg film data [18]. The dispersion of Ag powder was visualized by electron back-scatter diffraction (EBSD) mapping analysis system (Opal EBSD, Oxford) attached to a JEOL JSM-6700F scanning electron microscope. The average particle sizes of the commercial precursor $LiCoO_2$ and the $LiCoO_2$/Ag composite were determined by a JL1177 laser powder analyzer.

The charge and discharge capacities were measured with a coin cell, in which a lithium metal foil was used as the counter electrode. The electrolyte employed was 1 M $LiPF_6$ in ethylene carbonate and dimethyl carbonate solution (EC + DMC) (1:1). Cell assembly was carried out in an argon-filled glove box (NAC AM-2). The coin cells were cycled under different current densities between 4.4 and 3 V with a CT2001A cell test instrument (LAND Electronic Co.) at room temperature. Complex impedance measurements were carried out using a Solartron 1260 impedance analyzer in the frequency range of 10^{-1}–10^{7} Hz. A Solartron Model 1287 Electrochemical Interface was used for cyclic voltammogram measurements.

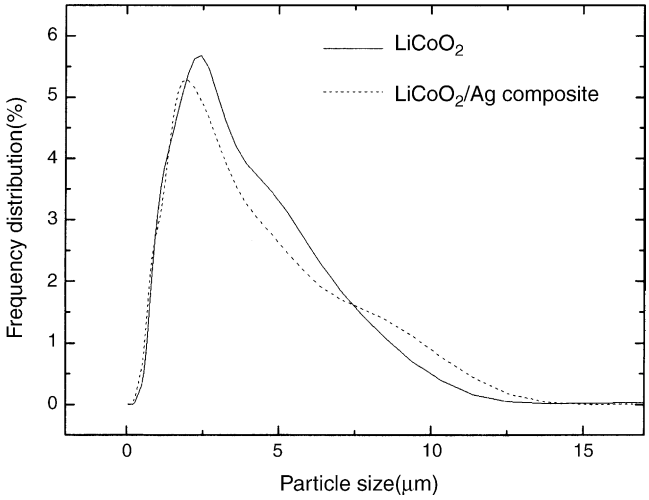

Fig. 1. The particle size distribution of (a) precursor $LiCoO_2$ and (b) $LiCoO_2$/Ag composite.

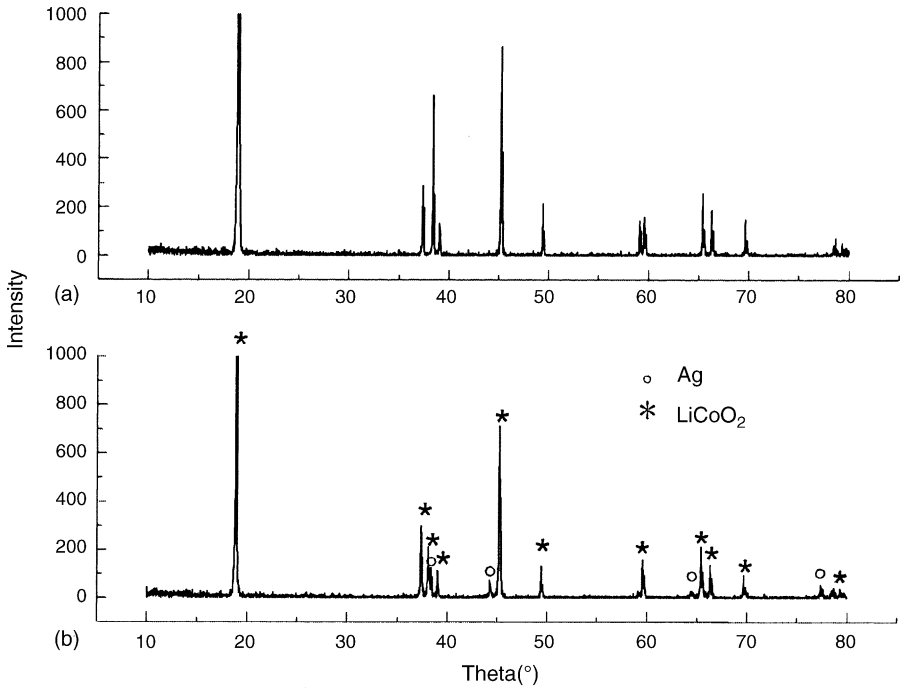

Fig. 2. XRD patterns of (a) precursor $LiCoO_2$ and (b) $LiCoO_2$/Ag composite.

3. Results and discussion

3.1. Characterization of the $LiCoO_2$/Ag composite particles

The particle-size distribution curves of the commercial precursor $LiCoO_2$ and the $LiCoO_2$/Ag composite were shown in Fig. 1. The average particle size of $LiCoO_2$/Ag composite was 2.8 μm, which was comparable to that of its precursor $LiCoO_2$ powder, 2.9 μm. The sizes of two powders were both in the range of 0.2–15 μm, which were in accordance with the EBSD images to be shown later.

Fig. 2 showed the XRD patterns of the commercial $LiCoO_2$ and the $LiCoO_2$/Ag composite. It was shown that except the characteristic patterns of Ag metal, all the peaks were in accordance with the patterns of $LiCoO_2$ precursor. The '*a*' and '*c*' values of the $LiCoO_2$ in the composite, 2.816 and 14.05 Å, were in accordance with those of the precursor $LiCoO_2$, i.e., $a = 2.817$ Å and $c = 14.05$ Å. Since the ionic radius of Ag (0.126 nm) was greatly bigger than that of the Co (0.063 nm), it was suggested that Ag did not enter the layered structure of $LiCoO_2$, the Ag containing specimen was just a composite of the Ag metal and $LiCoO_2$.

The EBSD images of the precursor $LiCoO_2$ and $LiCoO_2$/Ag composite were shown in Fig. 3. In the EBSD image of the $LiCoO_2$/Ag composite, it was clearly observed that Ag particles, the very small and white spots, were highly dispersed on the surface of $LiCoO_2$ powders. The size of the Ag particles was in the range of 10–100 nm. The Ag uniformly coated on $LiCoO_2$ might act as electronic conductor

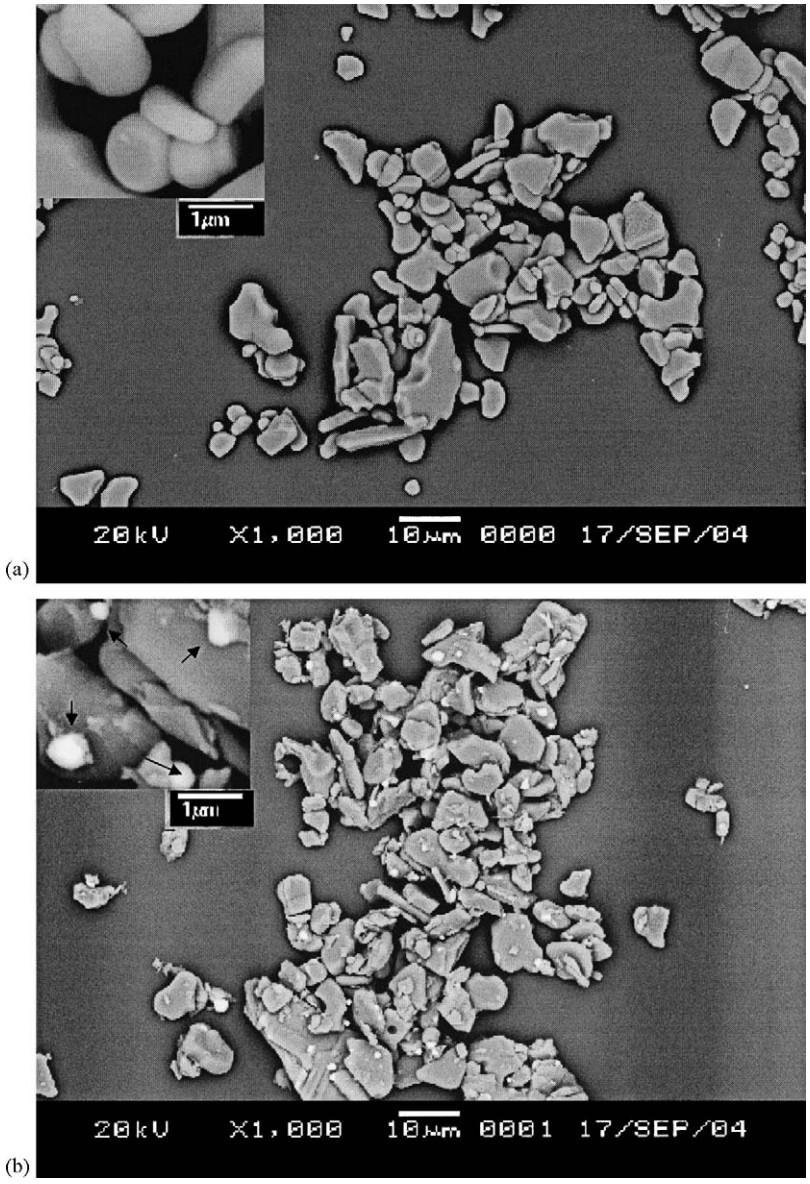

Fig. 3. EBSD images of (a) precursor $LiCoO_2$ and (b) $LiCoO_2$/Ag composite, where the bright and dark grains are corresponding to Ag particles and $LiCoO_2$, respectively.

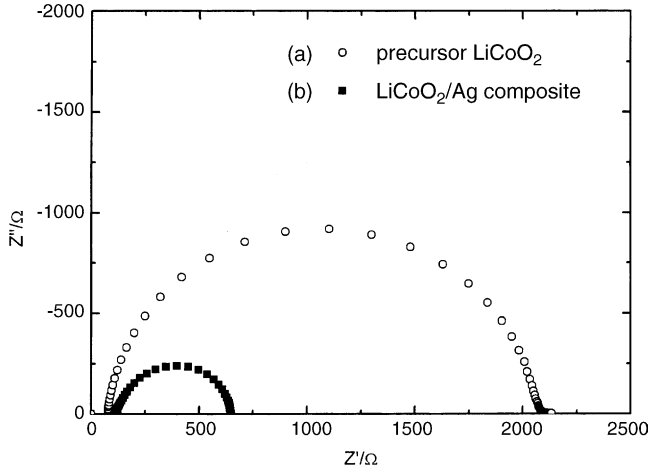

Fig. 4. Complex impedance plots at room temperature for (a) precursor $LiCoO_2$ and (b) $LiCoO_2$/Ag composite.

to enhance the surface intercalation reaction because of its relatively low resistance, which would be proved later in the ac impedance spectroscopy.

3.2. Electrical properties of the $LiCoO_2$/Ag composite

The conductivity of the specimen was determined from the ac impedance spectroscopy at ambient temperature. Fig. 4 showed the complex impedance plots of precursor $LiCoO_2$ and the $LiCoO_2$/Ag composite. According to the formula $s = d/AR$, the conductivity values were 7.25×10^{-5} and 2.31×10^{-4} S cm^{-1} for $LiCoO_2$ and the $LiCoO_2$/Ag composite, respectively. Since Ag did not enter the layered structure and the Ag containing specimen was just a composite, the increase of the conductivity in the $LiCoO_2$/Ag composite was mainly ascribed to the increase of the electronic conductivity.

The electrochemical behaviors of the $LiCoO_2$/Ag composite prepared in this work were characterized by cyclic voltammograms with coin cell. As shown in Fig. 5, the voltage was scanned from 3 to 4.5 V, and then back to 3 V at the scan rate of 0.5 mV s^{-1}. It was shown that an oxidation peak at about 3.9 V was found in addition to the characteristic peaks of $LiCoO_2$ in the first cycle but the corresponding reduction peak was not observed. Since the difference of standard electrode potentials between Li^+/Li and Ag^+/Ag is 3.85 V ($Li^+ + e = Li$ at −3.045 V and $Ag^+ + e = Ag$ at 0.7991 V), the oxidation peak probably will be attributed to the dissolution of silver. It was noteworthy that the silver content was difficult to enter the $LiCoO_2$ structure according to the XRD diffraction results and the oxidation peak ascribed to the Ag^+/Ag couple disappeared from the second cycle. The further works are underway to understand the cycling process of the $LiCoO_2$/Ag composite.

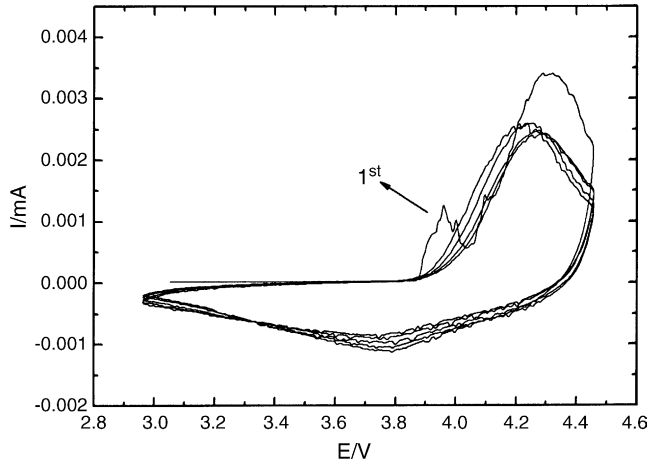

Fig. 5. Cyclic voltammograms of cells using the $LiCoO_2$/Ag composite as the cathode. Scan rate: 0.5 mV s^{-1}.

3.3. High-rate cycling performance of $LiCoO_2$/Ag composite

High-rate cycling behavior is one of the most important electrochemical characteristics of a lithium ion battery required for EV. In the present study, cycling performances were determined at different rates from 1C to as high as 10C. For each cycling, the charge and discharge processes were performed at the same current densities (Fig. 6).

Discharge–potential curves for the first cycle of the precursor $LiCoO_2$ and the $LiCoO_2$/Ag composite at various discharge rates were shown in Fig. 5. The cut-off voltages were controlled at 4.4 and 3 V for all charge–discharge cycles. It was noticeable that much lower overpotential was observed in the $LiCoO_2$/Ag composite in comparison with the precursor $LiCoO_2$, especially at high rates, indicating that the Ag additive significantly reduced the polarization of the cathode/electrolyte interface in the cell. Moreover, the discharge capacity of the $LiCoO_2$/Ag composite was much higher than the precursor $LiCoO_2$ especially at high discharge rate. For example, the discharge capacity of the $LiCoO_2$/Ag composite for the first cycle was 172.3 and 133.1 mAh g^{-1} at 1C and 10C, respectively, while for the precursor $LiCoO_2$ was 137.6 and 113.1 mAh g^{-1} at the corresponding discharge rates.

The change in discharge capacities with charge–discharge cycle numbers for precursor $LiCoO_2$ and the $LiCoO_2$/Ag composite was presented in Fig. 7. It was found that the discharge capacities of the $LiCoO_2$/Ag composite were much higher than those of the precursor $LiCoO_2$ at all discharge rates.

For all of the samples, the discharge capacities decreased with cycling more or less. Although the capacity degradation of the $LiCoO_2$/Ag composite was bigger than the precursor $LiCoO_2$ at lower discharge rate, its absolute value of discharge capacity after 50 cycles was much higher than the precursor. Moreover, at high discharge rates, the discharge degradation of the $LiCoO_2$/Ag composite was considerably lower than the precursor. The discharge capacity of the $LiCoO_2$/Ag composite reached 126.6 mAh g^{-1} after 50 cycles with a capacity loss of only 4.88% while it decreased to 75.8 mAh g^{-1}

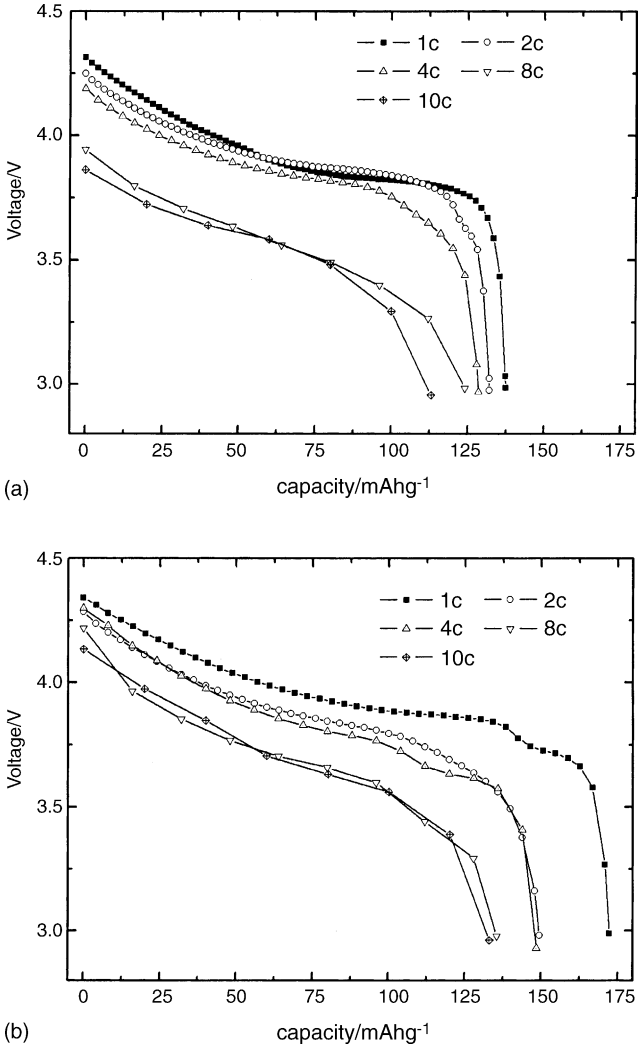

Fig. 6. The first discharge curves of the (a) precursor $LiCoO_2$ and (b) $LiCoO_2$/Ag composite between 3 and 4.4 V at different current densities.

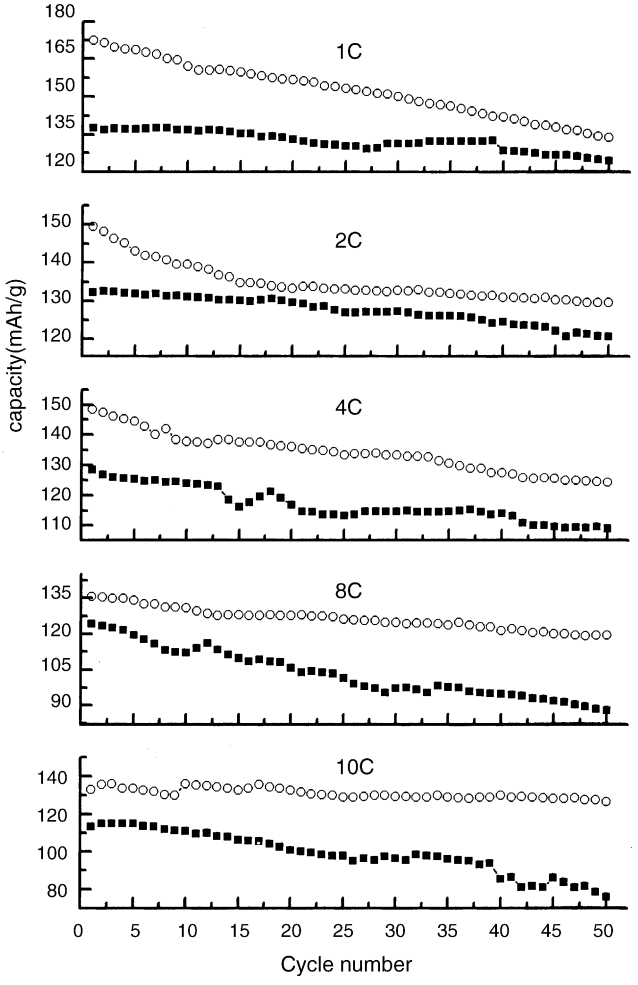

Fig. 7. Variation of the discharge capacities for (a) precursor $LiCoO_2$ and (b) $LiCoO_2$/Ag composite with the cycle number from 3 and 4.4 V at different current densities.

with a capacity loss as high as 32.98% for the precursor $LiCoO_2$ at 10C.

Table 1 summarized the cycling performances of the $LiCoO_2$/Ag composite in comparison with the precursor $LiCoO_2$ From the table, we could easily find that the reversible capacity of the $LiCoO_2$/Ag composite was much higher than the precursor $LiCoO_2$ at high charge–discharge rates. The discharge capacity after 50 cycles at 10C of the $LiCoO_2$/Ag composite, i.e., 126.6 mAh g^{-1}, reached nearly 95% of the capacity at 1C after 50 cycles. While for the precursor $LiCoO_2$, it was 75.8 mAh g^{-1} at 10C, only 61% of the capacity at 1C after 50 cycles. It was obvious that the Ag additive was significantly beneficial to the improvement of the reversible capacity and the cycling stability of the $LiCoO_2$ at high charge–discharge rates. As demonstrated by the cycling voltammetry, the Ag took part in the cycling process at least in the first cycle. The mechanisms for the greatly improved

Table 1
Summarization of cycling performance for precursor $LiCoO_2$ and the $LiCoO_2$/Ag composite

	Charge–discharge rate	1C	2C	4C	8C	10C
$LiCoO_2$/Ag composite	The second discharge capacity (mAh g^{-1})	172.3	149.5	148.5	135.6	133.1
	The 50th discharge capacity (mAh g^{-1})	133.9	129.7	124.3	119.4	126.6
	Capacity degradation (%)*	22.29	13.24	16.3	11.95	4.88
Precursor $LiCoO_2$	The second discharge capacity (mAh g^{-1})	137.6	132.2	128.6	124.1	113.1
	The 50th discharge capacity (mAh g^{-1})	124.7	120.7	109.1	88.1	75.8
	Capacity degradation (%)*	9.38	8.70	15.16	29.01	32.98

* Relative capacity loss compared to the second discharge.

high-rate cycling performance of the $LiCoO_2$/Ag composite are underway.

4. Conclusions

We have developed a simple method by using $AgNO_3$ as starting material to prepare the $LiCoO_2$/Ag composite cathode material for lithium ion batteries. The Ag additive has been demonstrated significantly beneficial to the reversible capacity and the cycling stability of the $LiCoO_2$ at high charge–discharge rate. The discharge capacity of the $LiCoO_2$/Ag composite was 133.1 mAh g^{-1} in the first cycle and remained 126.6 mAh g^{-1} in the 50th cycle at the rate of 10C, which was 40.13% higher than that of the precursor $LiCoO_2$.

Acknowledgment

This work was financially supported by key project of Natural Science Foundation of China (NSFC) No. 20333040.

References

[1] H.Y. Liang, X.P. Qiu, H.L. Chen, Z.Q. He, W.T. Zhu, L.Q. Chen, Electrochem. Commun. 6 (2004) 789–794.
[2] K.M. Abraham, D.M. Pasquariello, E.M. Willstaedt, J. Electrochem. Soc. 145 (1998) 482.
[3] K. Mizushima, P.C. Jones, P.J. Wiseman, J.B. Goodenough, Mater. Res. Bull. 17 (1980) 783.
[4] E. Plichta, S. Slane, M. Uchiyama, M. Saloman, D. Chua, W. Ebner, H. Lin, Solid State Ionics 136 (1989) 1865.
[5] H.F. Gibbard, J. Power Sources 26 (1989) 81.
[6] T. Nagura, K. Tazawa, Prog. Batteries Sol. Cells 9 (1990) 20.
[7] C.J. Patrissi, C.R. Martin, J. Electrochem. Soc. 146 (1999) 3176.
[8] H.L. Chen, X.P. Qiu, W.T. Zhu, P. Hagenmuller, Electrochem. Commun. 4 (2002) 488–491.
[9] H. Chen, X. Qiu, W. Zhu, P. Hagenmuller, Electrochem. Commun. 4 (2002) 488.
[10] N. Li, C.J. Patrissi, G. Che, C.R. Martin, J. Electrochem. Soc. 147 (2000) 2044.
[11] J.B. Bates, N.J. Dudney, B. Neudecker, A. Ueda, C.D. Evans, Solid State Ionics 135 (2000) 33.
[12] G.M. Ehrlich, C.M. Orndorff, R.M. Hellen, First Joint Meeting of the Electrochemical-Society/International-Society-of-Electrochemistry, Paris, France, August 31–September 5, 1997. Abst. No. 217.
[13] S. Hossain, in: D. Linden (Ed.), Handbook of Batteries, second ed., McGraw-Hill, New York, 1995, Chapter 36 and 37.
[14] D. Guyomard, J.M. Tarascon, Solid State Ionics 69 (1994) 222.
[15] Z.X. Shu, R.S. McMillan, J.J. Murray, J. Electrochem. Soc. 140 (1993) 922.
[16] S.H. Huang, Z.Y. Wen, X.J. Zhu, Z.H. Gu, Electrochem. Commun. 6 (2004) 1093–1097.
[17] J.T. Son, K.S. Park, H.T. Chung, H.-G. Kim, J. Power Sources 126 (2004) 182.
[18] P.E. Werner, Arkiv Fur Kemi 31 (1964) 513.